# Evolution of Flare Ribbons and Energy Release

Asai, A.[1], Masuda, S.[2], Yokoyama, T.[3], Shimojo, M.[3] Ishii, T.T.[1], Isobe, H.[1], Shibata, K.[1], and Kurokawa, H.[1] ; [1]Kwasan and Hida Observatories, Kyoto University, Japan, [2]Solar-Terrestrial Environment Laboratory, Nagoya University, Japan, [3]Nobeyama Radio Observatory, NAOJ, Japan,
Email (AA): asai@kwasan.kyoto-u.ac.jp

**Abstract**

We estimated the released magnetic energy via magnetic reconnection in the corona by using photospheric and chromospheric features. We observed an X2.3 flare, which occurred in active region NOAA9415 on 2001 April 10, in H$\alpha$ with the Sartorius Telescope at Kwasan Observatory, Kyoto University. Comparing the H$\alpha$ images with the hard X-ray (HXR) images obtained with *Yohkoh*/HXT, we see only two HXR sources which are accompanied by H$\alpha$ kernels. At these H$\alpha$ kernels the larger energy release is thought to be larger than at the other H$\alpha$ kernels. We estimated the energy release rates at each H$\alpha$ kernel by using the photospheric magnetic field strength and the separation speed of the H$\alpha$ flare ribbons at the same location. The estimated energy release rates at the H$\alpha$ kernels associated with the HXR sources are locally large enough to explain the different appearance. Their temporal evolution also shows peaks corresponding to HXR bursts.

## 1 Introduction

In the impulsive stage of solar flares, nonthermal electrons bombard the chromospheric plasma and cause HXR radiation. H$\alpha$ kernels, compact and bright points seen in H$\alpha$, are also generated by the precipitation of nonthermal electrons. Therefore, the light curves of H$\alpha$ kernels have a high correlation with those of the total HXR intensity, and each HXR source should be accompanied by H$\alpha$ kernels (Kurokawa, Takakura, & Ohki 1988). However, only a few H$\alpha$ kernels have their HXR counterparts, and the spatial distribution of H$\alpha$ kernels is different from that of HXR sources. We suggest that the lack of radiation sources in HXRs is caused by the low dynamic range of the HXR data. In the HXR images only the strongest radiation sources are seen, and the weaker sources are buried in noise.

The HXR intensity is proportional to the number of accelerated electrons, and is thought to be proportional to the energy release rate. The energy release rate is written as the product of the Poynting flux into the reconnection region $(4\pi)^{-1}B_c^2 v_i$ and the area of the reconnection region $A$ (Isobe et al. 2002) as follows;

$$\frac{dE}{dt} = \frac{B_c^2}{4\pi} v_i A, \qquad (1)$$

where $B_c$ is the magnetic field strength in the corona and $v_i$ is the inflow velocity into the reconnection region. We assume that the area $A$ does not change much during the flare so that $dE/dt \propto B_c^2 v_i$. To measure $B_c$ and $v_i$ directly is difficult. Here, we measure magnetic field strengths at the photosphere ($B_p$) instead of $B_c$, and the separation speed of the flare ribbons ($v_f$) instead of $v_i$ to estimate the energy release rates.

We observed a large two-ribbon flare (X2.3 on the GOES scale) which occurred in the NOAA Active Region 9415 at 05:10 UT, 2001 April 10 with the Sartorius Refractor Telescope (*Sartorius*) at Kwasan Observatory, Kyoto University (Fig. 1). Thanks to the short exposure time given for the flare, the H$\alpha$ images clearly show several bright kernels inside the flare ribbons without saturating. The details of the flare were reported in several papers (e.g. Asai et al. 2002a). We used HXR data taken with the hard X-ray telescope (HXT; Kosugi et al. 1991) aboard *Yohkoh* (Ogawara et al. 1991) to compare the locations of the HXR radiation sources with those of the H$\alpha$ kernels. The dynamic range of the HXT images is about 10. We estimated the energy release rates by using the $B_p$ and $v_f$ observed in Subsequently, we compared the energy release rates with the spatial distribution of the radiation sources in an HXR image. We also compared the temporal evolution of the energy release rates with the light curve of the HXR total intensity.

## 2 Evolution of Flare Ribbons and Energy Release

### 2.1 Magnetic Field Strength

Firstly, we examined the relation between the photospheric magnetic field strengths at each H$\alpha$ kernel and the energy release. We used a magnetogram obtained with the Michelson Doppler Imager (MDI; Scherrer et al. 1995) aboard the *Solar and Heliospheric Observatory* (*SOHO*; Domingo, Fleck, and Poland 1995) to measure the photospheric magnetic field strengths. We measured the magnetic field strength at each H$\alpha$ kernel (Fig. 1). We summarized the results in a previous paper (Asai et al. 2002b). The field strengths at the HXR sources (E2 and W2) are 3 times larger than the other H$\alpha$ kernels (Table 1).

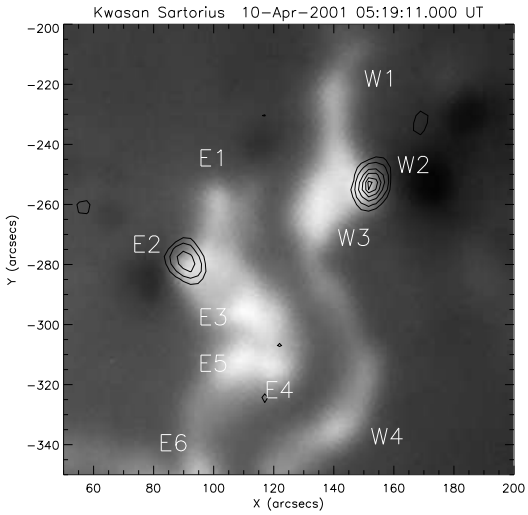


Figure 1: H$\alpha$ image taken with *Sartorius*. Solar north is up, and west is to the right. The HXR contour image is overlaid on it. Contour levels are 95, 80, 60, 40, 20 and 10% of the peak intensity. Ten H$\alpha$ bright kernels are numbered from E1 to E6 and from W1 to W4.

| kernel# | magnetic field strength (G) | HXR association |
|---|---|---|
| E1 | 260 | no |
| **E2** | **960** | **yes** |
| E3 | 240 | no |
| E5 | 230 | no |
| E6 | 220 | no |
| W1 | -500 | no |
| **W2** | **-1050** | **yes** |
| W3 | -260 | no |
| W4 | -300 | no |

Table 1: Photospheric magnetic field strengths at the H$\alpha$ kernels

If $v_i$ has no dependence on $B_c$, then eq. 1 indicates $dE/dt \propto B_c^2$. However, $dE/dt$ is thought to depend more significantly on $B_c$ since $v_i$ probably has some dependence on $B_c$ as some authors have suggested: from the model of Sweet (1958) and Parker (1957) we can derive the relation $v_i \propto B_c^{1/2}$ and hence $dE/dt \propto B_c^{5/2}$, alternatively, Petschek's model (Petschek 1964) suggests $v_i \propto v_A \propto B_c$ and hence $dE/dt \propto B_c^3$.

Here we used $B_p$ instead of $B_i$ as mentioned above. Since $B_p$ at the HXR sources is 3 times larger, these two models of magnetic reconnection predict that the energy release is 16 and 27 times stronger for the H$\alpha$ sources accompanied by

HXR sources than for the other H$\alpha$ kernels, respectively. This result indicates that a locally large energy release occurs at the HXR sources, and can explain the difference between the spatial distributions of the H$\alpha$ kernels and the HXR sources.

### 2.2 Separation of Flare Ribbons

Secondly, we examined the relation between the separation speed of the flare ribbons and the energy release. To do this, we compared the separation speed of the flare ribbons with the timing and the location of an HXR source. HXR sources appeared at different points at each HXR burst. We focused on the HXR burst which occurred at 05:22 UT. We drew the H$\alpha$ time slice image of the narrow slit superimposed on the H$\alpha$ kernel associated with the HXR source (Fig. 2). The separation speeds are determined as the temporal variation of the position of the ribbon-front. The timing of the HXR burst corresponds to the time when the separation speed of the flare ribbons reduces.

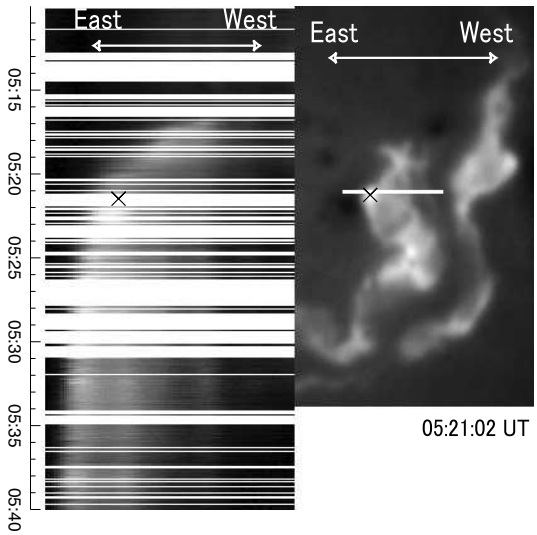


Figure 2: *Left*: Time slice image in H$\alpha$, which shows the separation of the eastern flare ribbon from the magnetic neutral line. *Right*: H$\alpha$ image overlaid with the slit. The crosses in both panels show the location of an HXR source and the time of the HXR burst.

From the magnetic reconnection model, the faster flare ribbons separate from each other, the greater magnetic flux participating in the magnetic reconnection, and hence the higher the expected energy release. Therefore, the fact that the HXR sources appear when the separation speed reduces seems to be inconsistent with the reconnection model. However, it is also known that the separation of flare ribbons is decelerated by strong magnetic field regions. Therefore, it is necessary to examine both the dependence of separation speed and magnetic field strength, simultaneously.

### 2.3 Reconnection Rate and Poynting Flux

Finally, we estimated the reconnection rate and Poynting flux by using $B_p$ and $v_f$, and compared them with the light curves in HXRs and microwaves. We put the slit on an H$\alpha$ kernel associated with the HXR source which occurred at 05:19 UT, like in §2.2. We estimated the temporal evolutions of the reconnection rate and the Poynting flux along the line, and compared the evolutions with the HXR light curve. The reconnection rate ($B_c \times v_i$) is written as $B_p \times v_f$ from the conservation of magnetic flux. The Poynting flux ($\propto B_c^2 \times v_i$) is more difficult to estimate. Here, we assumed that $B_c$ is proportional to $B_p$ in the same ratio all over the flaring region, and estimated the Poynting flux by using $B_p$ and $v_f$. If this assumption is correct, the differences in the energy release rates estimated with $B_p$ and $v_f$ are the same as those that would be obtained with $B_c$ and $v_i$.

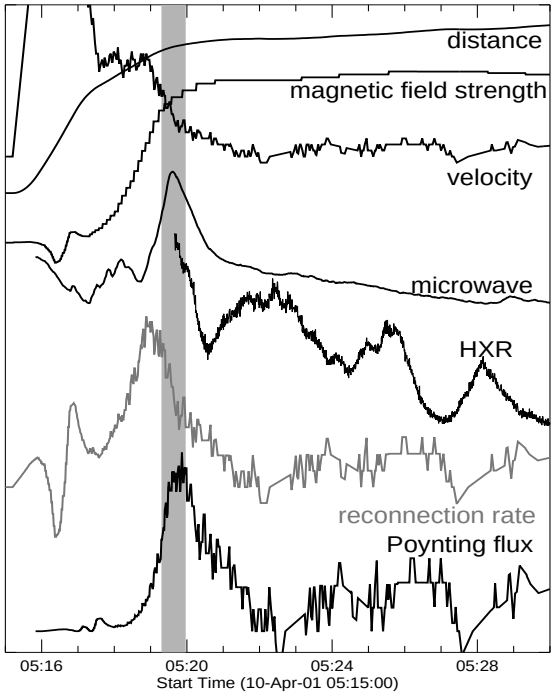


Figure 3: Evolution of the flare ribbons and energy release. All are plotted scaled arbitrarily. *From top to bottom*: Distance from the magnetic neutral line; photospheric magnetic field strength at the ribbon-front; separation velocity of the flare ribbon ($v_f$); light curve in microwaves; HXR count rate measured with HXT; estimated reconnection rate; estimated Poynting flux.

The evolutions of the reconnection rate and the Poynting flux are well fitted with the HXR light curve (see vertical light grey line in Fig. 3). The estimated reconnection rate and Poynting flux are large enough locally at the HXR sources that they can explain the difference between the spatial distribution of the HXR sources and that of the H$\alpha$ kernels.

**Acknowledgements**

We would like to thank all the members of Kwasan and Hida Observatories for their support during our observation, especially Ms. M. Kamobe who mainly performed the observation. We also thank Dr. D. H. Brooks for his careful reading and correction of our paper. The *Yohkoh* satellite is a Japanese national project, launched and operated by ISAS, and involving many domestic institutions, with multilateral international collaboration with the US and the UK. *SOHO* is a mission of international cooperation between the European Space Agency (ESA) and NASA.

**References**

Asai, A., Ishii, T. T., Kurokawa, H., Yokoyama, T., and Shimojo, M., 2002, ApJ, submitted
Asai, A., et al., 2002, ApJL, submitted
Domingo, V., Fleck, B., Poland, A. I., 1995, Sol.Phys., 162, 1
Isobe, H., et al., 2002, ApJ, 566, 528
Kosugi, T., et al., 1991, Sol.Phys, 136, 17
Kurokawa, H., Takakura, T., Ohki, K., 1988, PASJ, 40, 357
Ogawara, Y., et al., 1991, Sol.Phys., 136, 10
Parker, E. N., 1957, J. Geophys. Res., 62, 509
Petschek, H. E., 1964, in AAS-NASA Symp. on Solar Flares, ed. W. N. Hess (NASA SP-50), 425
Sweet, P. A., 1958, in IAU Symp. 6, Electromagnetic Phenomena in Cosmical Physics, ed. B. Lehnert (Cambridge: Cambridge University Press), 123
Scherrer, P. H., et al., 1995, Sol.Phys., 162, 129